AIDS RESEARCH AND HUMAN RETROVIRUSES
Volume 24, Number 8, 2008

DOI: 10.1089/aid.2008.0059

CD4$^+$ T-Cell Decline after the Interruption of Antiretroviral Therapy in ACTG A5170 Is Predicted by Differential Expression of Genes in the Ras Signaling Pathway*

Maryanne T. Vahey,[1] Zhining Wang,[2] Zhaohui Su,[3] Martin E. Nau,[2] Amy Krambrink,[3] Daniel J. Skiest,[4] and David M. Margolis[5]

Abstract

Patterns of expressed genes examined in cryopreserved peripheral blood mononuclear cells (PBMCs) of seropositive persons electing to stop antiretroviral therapy in the AIDS Clinical Trials Group Study A5170 were scrutinized to identify markers capable of predicting the likelihood of CD4$^+$ T-cell depletion after cessation of antiretroviral therapy (ART). A5170 was a multicenter, 96-week, prospective study of HIV-infected patients with immunological preservation on ART who elected to interrupt therapy. Study entry required that the CD4 count was greater than 350 cells/mm^3 within 6 months of ART initiation. Median nadir CD4 count of enrollees was 436 cells/mm^3. Two cohorts, matched for clinical characteristics, were selected from A5170. Twenty-four patients with an absolute CD4 cell decline of less that 20% at week 24 (good outcome group) and 24 with a CD4 cell decline of >20% (poor outcome group) were studied. The good outcome group had a decline in CD4$^+$ T-cell count that was 50% less than the poor outcome group. Significance analysis of microarrays identified differential gene expression (DE) in the two groups in data obtained from Affymetrix Human FOCUS GeneChips. DE was significantly higher in the poor outcome group than in the good outcome group. Prediction analysis of microarrays (PAM-R) identified genes that classified persons as to progression with greater than 80% accuracy at therapy interruption (TI) as well as at 24 weeks after TI. Gene set enrichment analysis (GSEA) identified a set of genes in the Ras signaling pathway, associated with the downregulation of apoptosis, as significantly upregulated in the good outcome group at cessation of ART. These observations identify specific host cell processes associated with differential outcome in this cohort after TI.

Introduction

The lifesaving advantages of antiretroviral therapy (ART) are evident. So too are the challenges faced by persons who fail therapy, experience significant adverse side effects from treatment, or suffer treatment fatigue. As more is learned about ART and treatment modalities evolve, persons who initiated ART under previous guidelines to "hit early and hit hard" would not currently be placed on ART.[1,2] At the other end of the spectrum are persons whose treatment options are crucially narrowed due to multidrug resistance or drug-related toxicities. Several studies have evaluated therapy interruption (TI) in closely monitored clinical trials involving primarily chronically infected persons on sustained ART with stable suppression of viremia and preserved CD4$^+$ T-cell counts (generally above 350 cells/μl).[3–7] In addition to possibly alleviating the significant clinical side effects and other burdens of prolonged ART, TI was initially postulated to induce the emergence of a more drug-sensitive virus (wild type) in persons with multidrug resistance[8,9] or

[1]Division of Retrovirology, The Walter Reed Army Institute of Research, Rockville, Maryland 20850.
[2]The Henry M. Jackson Foundation for the Advancement of Military Medicine, Rockville, Maryland 20850.
[3]Statistical and Data Analysis Center, Harvard School of Public Health, Boston, Massachusetts.
[4]Baystate Medical Center, Springfield, MA and Tufts University School of Medicine, Medford, Massachusetts.
[5]The Department of Medicine, University of North Carolina at Chapel Hill, Chapel Hill, North Carolina.
*The opinions or assertions contained herein are the private views of the authors, and are not to be construed as official, or as reflecting the views of the Department of the Army or the Department of Defense. None of the authors has commercial or other associations that might pose a conflict of interest. The Affymetrix data sets used to derive the observations discussed in this article can be accessed at: http://www.ncbi.nlm.nih.gov/geo/ under the accession numbers: GSE 10924.

in an increase in HIV-specific immunity following cycles of TI.[10–13] Enhanced HIV-specific immune response, mediated by the expansion of $CD8^+$ T cells, was postulated to enhance T-cell turnover rates[14] and speed of viral clearance,[11] lower viral set point, and/or to delay viral rebound, even if temporarily.[7,12,15]

Encouraging observations reporting modest association between increased HIV-specific $CD8^+$ memory cells and suppression of viral replication in the earliest trials of TI[16,17] involving small numbers of persons were discounted as the preponderance of evidence from larger studies in chronically infected persons with several rounds of TI of varying duration failed to define clear benefits of TI.[5–7,12,13,15,18–20] TI in acute or early HIV infection was associated with similar viral rebound.[10,21] Explanations for these observations include the failure of the transient and modest HIV-specific immunity and the associated expansion of $CD8^+$ T cells generated by TI to generate an effective long-term control of viral replication.[11,12,15] Additionally, reservoirs of persistent replication competent virus may be preserved even during sustained ART and emerge during TI.[10,13,15] Concomitant with viral rebound following TI, drug-resistant variants may emerge.[22]

Transient increases in $CD4^+$ T cells, modest expansion of viral-specific immunity, the fleeting emergence of wild-type virus, and some association with a temporarily lowered rate of clinical progression are seen after TI in some studies. However, the repercussions of viral rebound and the inability of the TI-associated immune response to result in a substantial and durable reduction in viral set point make the use of TI untenable in the clinical management of seropositive persons.[23] The SMART study, the largest interventional study conducted in HIV-seropositive persons, recently revealed that TIs are associated with a significant increase in risk of morbidity and mortality from events, many cardiovascular in nature, not previously considered to be HIV-associated and suggested that there was no benefit associated with TI in any subpopulation of patients in the study.[24]

Nevertheless, in the context of research to identify correlates of disease progression, samples derived from TI clinical studies have the potential to provide critical information on the performance and utility of the gold standard correlates of HIV disease progression, such as $CD4^+$ T-cell levels, viral load, and definitive clinical endpoints, as they can be assessed dynamically, in the short term, and in the context of extensive clinical evaluation. Importantly, these well-documented clinical studies also offer the opportunity to evaluate new and novel approaches to the assessment of risk of disease progression. The identification of biomarkers, in turn, builds the collection of tools for the assessment of both drug interventions for the control of HIV disease and the performance of vaccines for the prevention of HIV disease.

We studied samples from persons enrolled in a TI trial, ACTG 5170, which determined that the incidence of clinical endpoints was reduced and that the time to these endpoints was prolonged in persons with higher $CD4^+$-cell nadir on ART, lower viral loads prior to ART, and a viral load below detection at TI.[6] We sought to determine if patterns of gene expression in the peripheral blood mononuclear cell (PBMC) compartment, a type of sample consistently and easily available from clinical studies, might be correlated with the course of disease upon TI. Our findings identified specific host-cell processes in the PBMC compartment that are associated with differential outcome after TI.

Materials and Methods

Clinical specimens

PBMCs were obtained with informed consent from study volunteers enrolled in ACTG 5170, a multicenter clinical trial approved by local human use institutional review boards. Eligibility criteria for ACTG 5170 included confirmed HIV-1 infection, age > 12, CD4 count > 350 cells/mm^3 immediately prior to first ART, CD4 count > 350 cells/mm^3, plasma HIV-1 RNA viral load $< 55{,}000$ copies/ml at screening, currently receiving ART with ≥ 2 drugs for ≥ 6 months, and Karnofsky score ≥ 70.[6]

A5170 was a multicenter, 96-week, prospective study of HIV-infected patients with immunological preservation on ART who elected to interrupt therapy. Study entry required that the CD4 count was greater than 350 cells/mm^3 within 6 months of ART initiation. Median nadir CD4 count of enrollees was 436 cells/mm^3. Two cohorts, matched for clinical characteristics, were selected from A5170. Twenty-four

Table 1. Descriptive Statistics for the Study Groups

Statistic	*Good outcome group* (n = *24*)	*Poor outcome group* (n = *24*)[a]	*p values*
CD4 cells at week 0	798.35 ± 224.30	900.71 ± 236.46	0.146
CD4 cells at week 24	675.13 ± 212.31	499.54 ± 165.45	4.00×10^{-3}
Delta CD4 cells	−123.23 ± 127.31	−401.17 ± 204.05	1.22×10^{-7}
Viral load at week 0	1.716 ± 0.064	1.726 ± 0.067	0.157
Viral load at week 24	3.467 ± 0.832	4.432 ± 0.828	5.96×10^{-4}
Delta viral load	1.716 ± 0.856	2.705 ± 0.817	6.43×10^{-4}
Gender	23 M/1F	22 M/2 F	
Age	41.50 ± 8.85	41.00 ± 6.71	0.650

Values are the mean ± the standard deviation. *p* values were determined using the Wilcoxon rank-sum test. Viral load is expressed as $\log_{10}$ copies of viral RNA per milliliter of plasma. Values of viral load below the assay cut off of 50 copies were scored as 50 copies. $CD4^+$ T-cell levels are expressed as number of cells per milliliter.

[a]Clinical data for two of the samples in the poor outcome group were taken at week 12 and 16 and for one of the samples in this group at week 4. GeneChip data was within 6–8 weeks of the clinical data. One sample in the poor outcome group had both clinical and GeneChip data from week 32.

patients with an absolute CD4 cell decline of less that 20% at week 24 (good outcome group) and 24 with a CD4 cell decline of >20% (poor outcome group) were studied. The good outcome group had a decline in $CD4^+$ T-cell count that was 50% less than the poor outcome group. The good outcome group never reinitiated ART over the course of the study while nine persons in the poor outcome group reinitiated ART at a $CD4^+$ T-cell decline of >40%. PBMCs were collected by Histopaque-Ficoll (Sigma, St. Louis, MO) gradient centrifugation and were cryopreserved. Samples were assessed for gene expression patterns at the time of cessation of ART (week 0 in our study) and at 24 weeks after TI.

Standard measures of disease progression

The Roche Amplicor HIV Monitor test (version 1.5: Roche Diagnostics, Basel, Switzerland) was used to determine plasma viral load.

Peripheral blood lymphocyte subset analysis was performed on a FACS Calibur flow cytometer (Becton-Dickinson, Mountain View, CA) using a panel of mouse anti-human monoclonal antibodies according to the manufacturer.

Gene expression profile analysis using Affymetrix GeneChips

Preparation of cellular RNA and subsequent processing for GeneChip analysis were performed as described previously[25] using the Agilent 2100 Bioanalyzer system (Agilent Technologies, Santa Clara, CA) to assess the integrity and quantity of RNA and the Affymetrix Human Focus GeneChip (Affymetrix, Santa Clara, CA). This platform consists of 8700 probe sets and assesses 8500 transcripts for 8400 full-length and fully annotated genes.

GeneChips with a scaling factor greater than 50 and an array outlier percentage greater than 5% on dCHIP2005[26] were

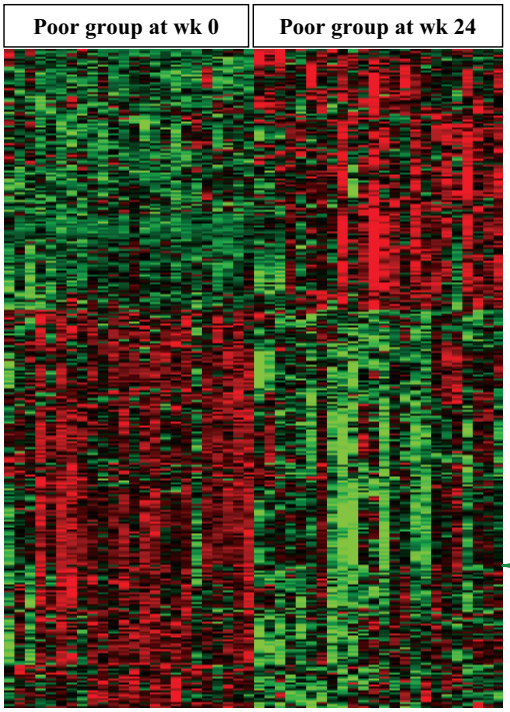

Functional categories of 133 up regulated genes	No. of genes	p values
Response to virus	12	4.58E-11
M phase of mitotic cell cycle	9	3.44E-05
Mitotic sister chromatid segregation	4	6.28E-04
Regulation of progression through cell cycle	12	1.57E-03
Inflammatory response	8	1.81E-03
Innate immune response	5	2.39E-03
Chemotaxis	6	3.65E-03
Regulation of apoptosis	9	8.80E-03
Regulation of programmed cell death	9	9.09E-03
DNA metabolism	13	9.15E-03
Cellular defense response	5	1.06E-02
Humoral immune response	6	1.15E-02
Positive regulation of programmed cell death	6	1.15E-02
Humoral defense mechanism	5	1.62E-02
Apoptosis	11	1.67E-02
Cation homeostasis	5	1.90E-02
Complement activation	3	3.64E-02

Functional Categories of 208 down regulated genes	No. of genes	p values
Protein biosynthesis	58	2.13E-26
Macromolecule biosynthesis	59	5.33E-25
Cellular protein metabolism	75	6.07E-07
Regulation of protein biosynthesis	7	9.28E-03
Regulation of cellular biosynthesis	7	1.14E-02

Functional categories of 51 up regulated genes	No. of genes	p value
response to virus	5	8.18E-05
cellular defense response	4	3.35E-03
biopolymer catabolism	5	5.16E-03
protein catabolism	4	2.80E-02

FIG. 1. Differential gene expression at 24 weeks after cessation of ART. (**A**) Differential expression in poor outcome group. There were 133 genes upregulated and 208 genes downregulated at significant level of false discovery rate (FDR) < 1%. On the left is a heat map showing the magnitudes of gene expression changes (see Supplementary Table 1 for expression values of each gene in each sample). Gene ontology (GO) categories of these 133 up- and 208 downregulated genes are shown on the right. Only categories whose p values are less than 0.05 are listed. The p values of each GO category were determined by the online tool, DAVID. (**B**) Differential expression in the good outcome group. Unlike the poor outcome group, the number of differentially expressed genes in the good outcome group was much less. There were only 51 genes upregulated from week 0 to week 24 at FDR < 1% significant level, and no genes downregulated at FDR < 1% significant level.

eliminated from further analysis. CEL files were normalized at the probe level using the robust multichip average method[27] built into the BioConductor package Affy-1.12.2. Genes scored as absent in all 96 samples were eliminated from analysis.

The Affymetrix datasets used to derive the observations discussed in this article can be accessed at: http://www.ncbi.nlm.nih.gov/geo/ under the accession numbers: GSE 10924.

Gene expression data analysis methods

Differentially expressed genes were identified by using the statistical program Significance Analysis of Microarrays (SAM) version 3.0[28] and cluster analysis of microarray datasets was performed using MultiExperiment Viewer available at http://www.tigr.org/software/microarray.shtml. SAM identifies genes whose expression has significantly changed by leveraging a set of gene-specific *t* tests. Genes are assigned a score derived from the change in expression relative to the standard deviation for all measurements made for that gene. Genes that exceed a threshold are scored as statistically significant. The percentage of genes being called significant by chance is measured by false discovery rate (FDR). We used a cutoff of FDR $< 1\%$ for SAM, which is very stringent.

The functions and biological classifications of differentially expressed genes were analyzed by the web-based tool, DAVID, which sorts gene lists into functional profiles using broad gene ontology categories by associated biological processes.[29] Ontology groupings for genes overlap by nature of the fact that the products of genes may have multiple functions.

Class prediction was performed using an academic software package, Prediction Analysis of Microarray with R (PAM-R), which implemented the nearest shrunken centroid algorithm.[30] The software provides a k-fold cross-validation method to estimate the predicting capability of the resultant classifier set of genes. PAM-R is available at http://www.bioconductor.org. PAM-R is an iterative analytical method that uses sets of individual genes, called classifier sets, that together are capable of assigning samples to a given group.

Gene set enrichment analysis (GSEA) or R-GSEA and MSigDB (Molecular Signatures DataBase of gene sets) were used to identify differentially expressed sets of genes. Both the software and geneset database were downloaded from the website of The Broad Institute of MIT and Harvard (http://www.broad.mit.edu). GSEA identifies sets of related genes, as opposed to individual genes, associated with biological pathways that are coregulated and are associated with progression after TI in our study. We used GSEA's default statistical cutoff FDR < 0.25.

Independent confirmation of GeneChip expression data

To confirm observations from the gene chip data, TaqMan® Gene Expression Assays (Applied Biosystems, Foster

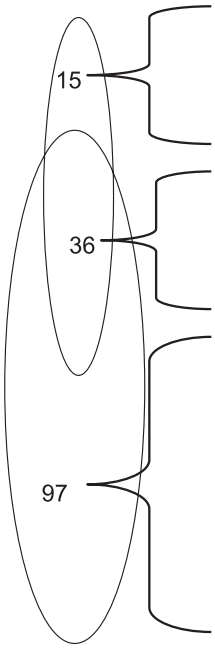

Functional categories of 15 genes unique in good outcome group	No. of genes	p values
Biopolymer catabolism	4	0.001087564
Protein catabolism	3	0.016571123
Cellular macromolecule catabolism	3	0.037432451

Functional categories of 36 genes common to both groups	No. of genes	p values
Response to virus	5	1.57E-05
Cellular defense response	4	0.001020
Nucleotide biosynthesis	3	0.040293

Functional categories of 97 genes unique to poor outcome group	No. of genes	p values
Response to virus	7	1.00E-05
M phase of mitotic cell cycle	7	3.51E-04
Mitotic sister chromatid segregation	3	0.007269
Regulation of progression through cell cycle	9	0.008299
Positive regulation of programmed cell death	5	0.019083
Apoptosis	9	0.022421
Regulation of apoptosis	7	0.022696
Regulation of programmed cell death	7	0.023250
Chemotaxis	4	0.042513
Inflammatory response	5	0.042730

FIG. 2. Survey of the distribution of genes significantly upregulated in the poor and good outcome groups. The numbers of genes in the ontological groups as determined by DAVID are given as well as the associated *p* values for each. Common to both groups were genes associated with viral infection. Distinct in the poor and good outcome groups were genes associated with catabolism and in the poor group were those associated with apoptosis, programmed cell death, and progression through the cell cycle.

City, CA) optimized for microarray validation (*3′ most*) were used to detect NFKB1, RELA, RAF1, and PIK3CA in three randomly chosen, matched sets of good and poor outcome samples. The fluorescence signals were measured in real time using ABI HT7900 and critical threshold (CT) values were output from the software SDS2.1. Glyceraldehyde 3-phosphate dehydrogenase was used as internal control to calculate fold changes of target genes in good versus poor outcome samples by the $2^{-\Delta\Delta CT}$ method.

Results

Demographic and clinical characteristics of the study group

There were 96 samples in the study set. Table 1 summarizes the characteristics of the good and poor outcome groups at week 0 (at cessation of ART) and 24 weeks later. The drop in $CD4^+$ T cells in the samples in the good outcome group was 50% less than the corresponding matched sample in the poor

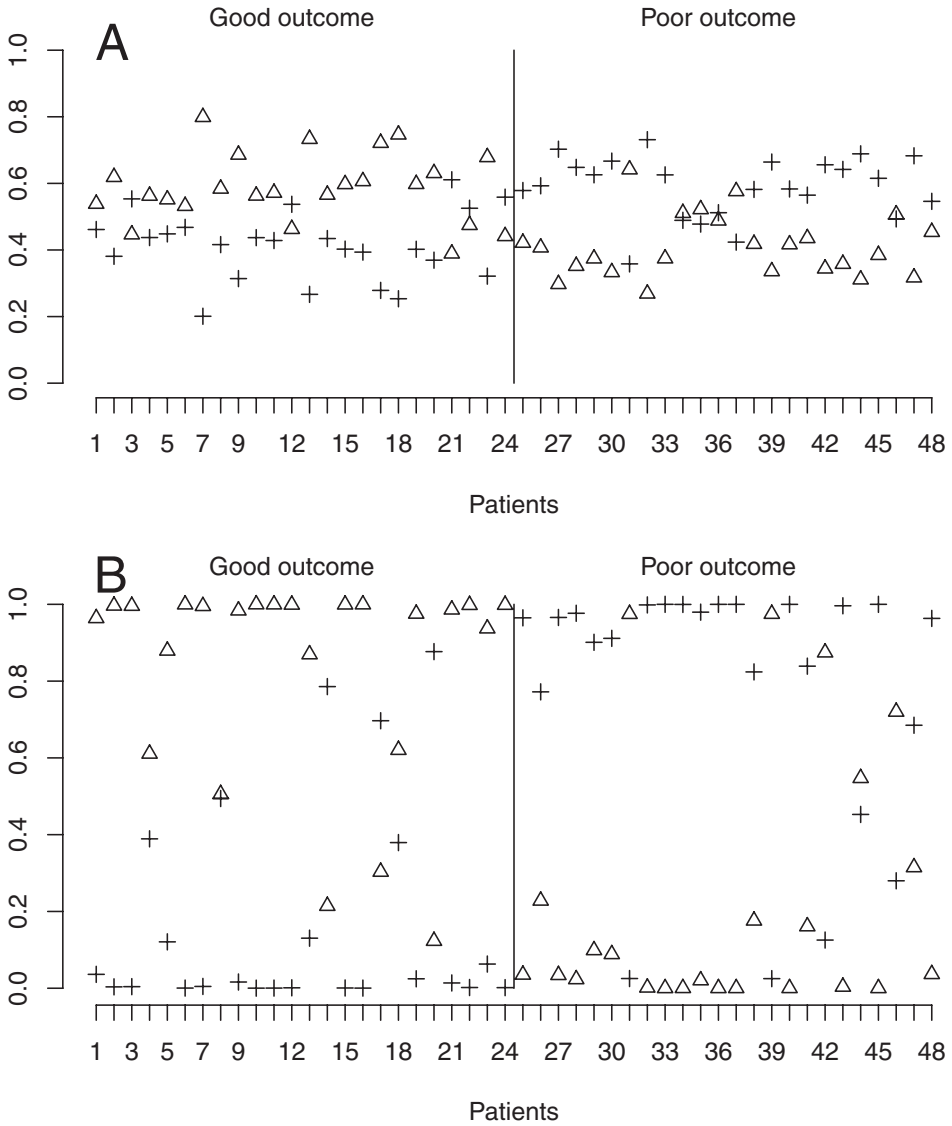

FIG. 3. Classification analysis for outcome at week 0 and at week 24 after the cessation of antiretroviral therapy. (**A**) Prediction analysis of microarrays (PAM-R) analysis of classification and prediction at week 0 showing an 81% accuracy in classification by the 53 genes in the classifier set. (**B**) PAM-R analysis of classification and prediction at week 24 showing an 83% accuracy in classification by the 176 genes in the classifier set. The *x*-axis (numbers 1 through 48) shows the patients in the analysis with numbers 1–24 belonging to the good outcome group and numbers 25–48 to the poor outcome group. For each patient, there are two symbols. A triangle indicates the probability, shown on the *y*-axis, of a patient being predicted to belonging in the good outcome group, and a cross indicates the probability of the same patient being predicted as belonging to the poor outcome group. If a triangle is above a cross, the patient is classified as belonging to the good outcome group and conversely, if a cross is above a triangle, the patient is classified as belonging to the poor outcome group. For a given patient, the sum of all probabilities is always equal to 1.

outcome group. The good outcome group was characterized by a mean loss of 123.23 cells over the study period, and the poor outcome group by a mean loss of 401.17 cells (Wilcoxon rank-sum test, $p = 1.22 \times 10^{-7}$). At study entry, the two groups had no significant difference in plasma viral load, $CD4^+$ T-cell levels, or age. At week 24, there was a significant difference between the two groups in $CD4^+$ T cells, viral load, and the mean change in both these parameters since study entry. The groups do not differ in gender or race as 94% were male, 6% female and 67% were Caucasian, 19% were African-American, 10% Hispanic, and 4% Asian/Pacific Islander. There was no significant difference in the ART history in the two groups (data not shown). Principal component analysis indicated that expression profiles of samples in the poor outcome group taken at weeks 4, 12, 16, and 32 were not outliers.

Differential gene expression is associated with progression after the cessation of ART

SAM using study entry (week 0) as baseline, with an FDR of 1%, was used to identify genes that exhibited a significant change in expression level over the 24-week study period.

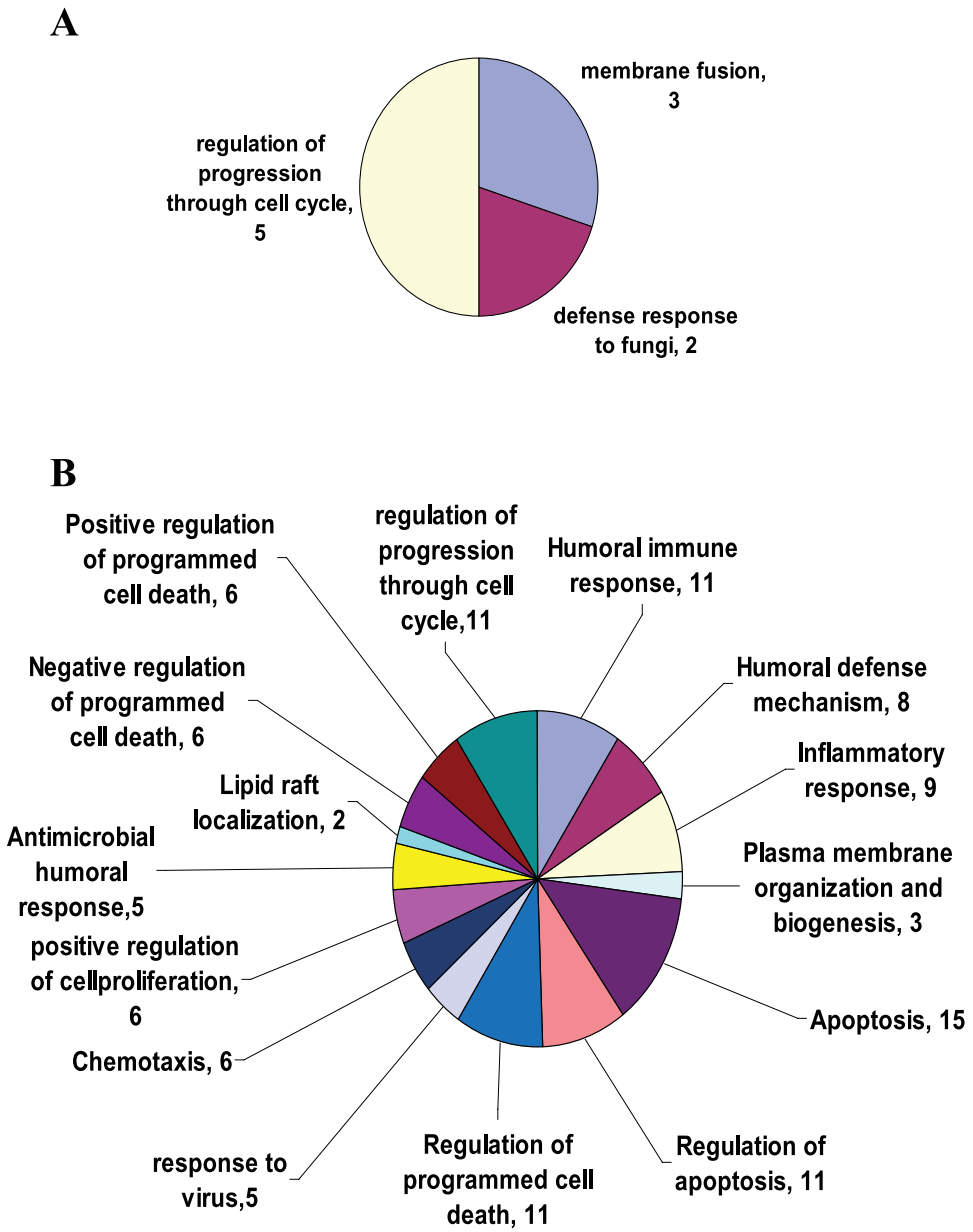

FIG. 4. Functional categories of genes comprising the classification sets at week 0 and at week 24. (**A**) Pie chart of those functional categories in the classifier set at week 0 that were annotated by DAVID at biological process level 5. Genes associated with progression through the cell cycle are included. (**B**) Pie chart of those functional categories in the classifier set at week 24 that were annotated by DAVID. Genes associated with the regulation of apoptosis and cell cycle predominated. Only genes with p value of < 0.05 are shown.

Differentially expressed (DE) genes were annotated using the DAVID database to determine significantly enriched gene ontology (GO) functional categories with a cutoff p value of 0.05. The complete list of differentially expressed genes is given in the Appendix.

More differential expression was observed in the poor outcome group over the study period than in the good outcome group at an FDR of 1%. Figure 1 is a heat map showing the upregulation of 133 genes and the downregulation of 208 genes in the poor outcome group over the 24-week period. Also shown are the remarkably few genes, 51 upregulated and no significantly downregulated genes, whose expression was significantly changed over the study period in the good outcome group. Corresponding GO functional categories are also shown. Genes associated with response to viral infection were among those upregulated. The DE genes that were downregulated at week 24 were dominated by those associated with biosynthesis and metabolism.

In the good outcome group, 51 genes were differentially expressed over the study period and none were downregulated. Genes associated with response to viral infection and cellular defense predominated the set of upregulated genes in the good outcome group.

Figure 2 displays a Venn diagram of the differences and similarities between DE in the good and poor outcome groups in genes that are upregulated over the 24-week period. There were 15 genes that were upregulated and were unique to the good outcome group. Thirty-six upregulated genes were observed in both outcome groups, and 97 upregulated genes were unique to the poor outcome group. The major functional categories that comprise the upregulated genes shared by both groups were those associated with response to virus (five genes) and with cellular defense response (four genes). Functional categories unique to the poor outcome group included apoptosis, inflammatory response, and the positive regulation of programmed cell death, and those associated with catabolism were uniquely upregulated in the good outcome group.

DE of sets of genes is capable of classifying patients as to progression after the cessation of ART with greater than 80% accuracy

PAM-R was used to leverage a 10-fold cross-validation method to identify sets of classifier genes capable of sorting samples into good and poor outcome groups. Figure 3(A) and (B) show the results of PAM-R at study entry and week 24, respectively. The graph in Fig. 3(A) shows that, leveraging the expression of a distinct set of genes, samples can be assigned to the good or poor group with an overall accuracy of 81% at study entry. The resolution of the assignment of samples to the two groups increased significantly by 24 weeks, shown in Fig. 3(B), as indicated by the increase in the separation of the probability of assignment to the correct group shown on the ordinate. Figure 4(A) and (B) show pie charts of the known functional categories of the 53 genes comprising the 81% accurate classifier set at study entry and the 176 genes comprising the 83% accurate classifier set at week 24.

Of the genes in the 53 gene classifier set at study entry that can be annotated by DAVID and have a p value of less than 0.05, genes associated with the regulation of progression through the cell cycle were observed. In the 176 gene classifier set at week 24, genes associated with the regulation of apoptosis and progression through the cell cycle dominate and those associated with the immune re-

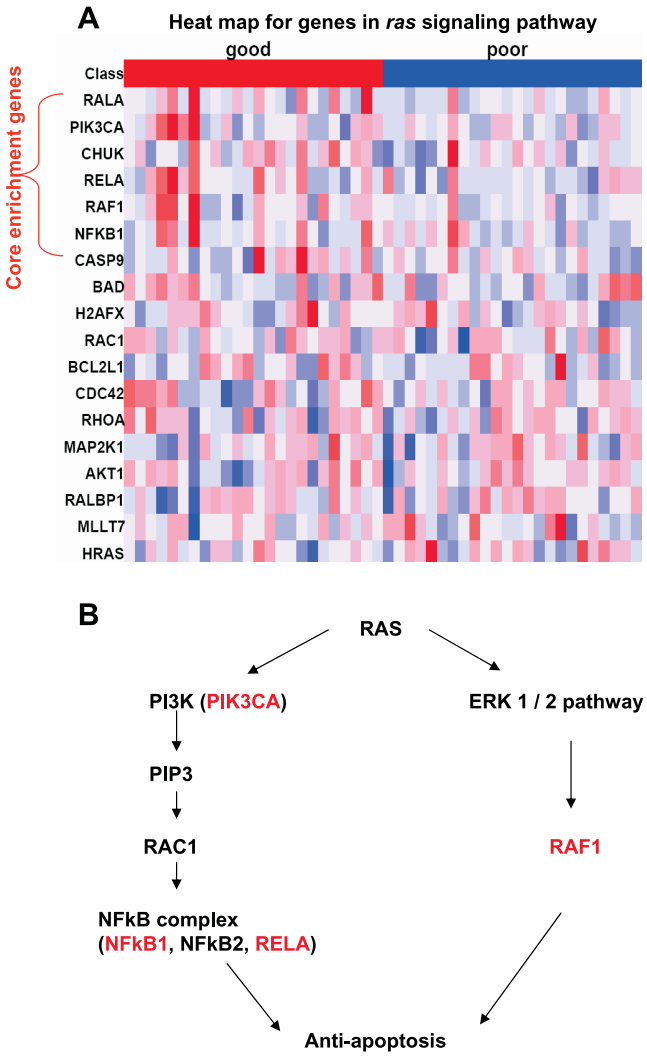

FIG. 5. Gene set enhancement analysis and identification of genes in the Ras signaling pathway associated with the regulation of apoptosis at week 0. (**A**). Heat map showing the differential expression of genes in the Ras signaling pathway in the two outcome groups. (**B**) Network of Ras signaling pathway genes identified by gene set enrichment analysis. The expression of genes whose annotations are given in red ink was independently confirmed by reverse-transcriptase polymerase chain reaction. ERK 1/2, extracellular signal regulated kinase; Ras, Regulator GTPase, rat sarcoma viral oncogene; PIK3 CA, phosphatidylinositol e kinase catalytic subunit A isoform; RAC1, Ras-related botulinum toxin substrate 1; PIP3 phosphoinositide binding protein 3; RAF1, v*raf* 1 murine leukemia viral oncogene homolog 1; NFKB1, nuclear factor of kappa light polpeptide gene enhancer in B cells 1; RELA, v*ref* reticuloendotheliosis viral oncogene homolog A.

sponse, viral infection, and proliferation are also represented.

High-resolution gene set enrichment analysis identified genes in the Ras pathway that are specifically associated with the downregulation of apoptosis and that are differentially enriched in samples from patients with good outcome

High-resolution gene set enrichment analysis was used to identify sets of genes known as "core enrichment genes," which are differentially expressed at week 0, the point of cessation of ART. The results of this analysis are shown in Fig. 5(A) and (B). Figure 5(A) displays a heat map showing the expression of the set of core enrichment genes in the Ras family that were identified by GSEA as being upregulated in the good outcome group. The Ras genes identified by GSEA were associated with the modulation of apoptosis. The functional pathway of these genes is shown in Fig. 5(B). The expression of genes whose annotations are shown in red ink in Fig. 5(B) were independently confirmed by reverse-transcriptase (RT) polymerase chain reaction (PCR).

Real-time PCR confirmed the expression of the genes in the Ras pathway that were upregulated in the good outcome group

Table 2 summarizes the confirmation by RT PCR of the DE in randomly chosen, matched samples from the good and poor outcome groups at the time of cessation of ART and identified by the expression data as genes associated with the regulation of apoptosis in the Ras signaling pathway. The correlation coefficient for the concordance of these two independent means of deriving the data was $r = 0.93$.

Discussion

The goal of this study was to ascertain if, prior to ART interruption, distinct patterns of gene expression might be associated with disease progression or outcome in persons who stop ART. A second goal of the study was to use these patterns to identify biological and cellular processes that might account for such an association. Clearly, the good and poor outcome groups were indistinguishable by demographic and traditional clinical features at the time of cessation of ART (week 0) and were by week 24 significantly divergent in clinical status. Accordingly, there are definitive patterns of gene expression associated with the two groups at week 24. Although this might be expected after clinical progression has occurred, the observation that gene expression patterns that are associated with outcome at week 24 can be identified at week 0 is highly significant.

Genes associated with apoptosis are shown by the three levels of analysis used in our study to be indicative of differential outcome. SAM analysis indicates that these genes are uniquely upregulated by week 24 in the poor outcome group. The more stringent classification analysis indicates that by week 24, genes associated with the regulation of apoptosis are represented in the 176 genes capable of classification of samples into two divergent groups with an accuracy of 83%. Classification analysis also indicates that there are patterns of gene expression that are capable of distinguishing the two groups at week 0. The analysis presented in Fig. 3(A and B) is critical for several reasons in that: (1) it demonstrates the degree to which expression profiles can distinguish differential outcome after TI and 24 weeks later and (2) it shows that such profiles can distinguish differential outcome as early as study entry when the traditional markers of $CD4^+$ T-cell levels and viral load are indistinguishable. In addition, this analysis provides the collection of genes that drive the prediction of outcome and that include those associated with the regulation of cell cycle and apoptosis as shown in Fig. 4(A and B). These data prompted the GSEA, which confirmed and extended the identification of the modulation of apoptosis as the underlining functional pathway that distinguished good and poor outcome persons.

The extensive scrutiny of gene expression at week 0 by GSEA identified a set of genes, as opposed to individual genes, that are associated with the regulation of apoptosis in the Ras signaling pathway. Independent confirmation of the differential expression data generated by gene chip analysis, using RT-PCR in both good and poor outcome samples, further substantiated the pivotal role of this gene family in disease course immediately after the cessation of ART. Taken together, these data indicated that the regulation of apoptosis may play a significant role in the pathogenesis of disease after the cessation of ART. Furthermore, as there appeared to be little difference in HIV pathogenesis after the initial establishment of viral set point following infection and after the reestablishment of viral set point following TI, the regulation of apoptosis may play an important role in HIV pathogenesis throughout the course of HIV infection. Observations in the nonhuman primate model report a species-specific, divergent immune response in a natural host (sooty mangabey) and a nonnatural host (rhesus macaque) that is evident from the time of infection with

Table 2. RT-PCR Confirmation of the Upregulation of *Ras* Signaling Pathway in Good Outcome Group at Week 0

PIK3CA		*RAF1*		*NFKB1*		*RELA*	
RT-PCR	*GeneChip*	*RT-PCR*	*GeneChip*	*RT-PCR*	*GeneChip*	*RT-PCR*	*GeneChip*
1.89	1.54	1.43	1.18	0.69	0.79	1.29	1.12
3.33	4.91	1.00	1.86	1.89	2.24	1.63	2.11
4.06	4.25	2.03	2.46	5.00	5.28	1.86	1.37

Values in the table are the fold changes of good versus matched poor samples. For each gene, the left column is fold change detected by RT-PCR and the right column is fold changes measured by GeneChip in three sets of samples. Correlation coefficient of GeneChip and RT-PCR data is 0.93. The fold change was calculated by $2^{-\Delta\Delta CT}$ method using GAPDH as internal control. RT, reverse-transcriptase; PCR, polymerase chain reaction.

uncloned simian immunodeficiency virus, sooty mangabey (SIVsm). Both hosts developed high levels of viremia but in the sooty mangabey, an attenuated immune response was correlated with an absence of $CD4^+$ T-cell decline and simian immunovirus (SIV)-associated pathogenesis. These observations suggest that the host response to infection plays a critical role in SIV, and by extension, HIV, pathogenesis.[31] Similar observations have been reported in three HIV-seropositive persons who are long-term nonprogressors.[32]

The Ras signaling pathway is the specific gene family associated by GSEA with differential outcome after TI. Ras, named for its association with rat sarcoma viral oncogenes, is an extensively studied small guanosine triphosphatase protein[33] that relays extracellular signals to intracellular signaling cascades. The protein plays a pivotal role in the complex positive and negative feedback loops that modulate cell survival and cell death, as well as cell proliferation and differentiation.[34–36] Understandably, this protein has been scrutinized by the oncology field as a potential drug target to halt the transformation and unchecked growth associated with cancer.[37] In our study, the cascade of the convoluted Ras signaling pathway that is associated with differential outcome after TI involved impingement on PI3K (also known as PIK3CA, phosphatidylinositol 3 kinase catalytic subunit, alpha isoform) and ERK (extracellular signal regulated kinase)/RAF 1 (v*raf*1 murine leukemia viral oncogene homolog 1). Among the myriad of regulatory pathways involving Ras, the pathway associated with good outcome in our study modulates antiapoptotic processes.[35,38,39] Gene expression patterns of PI3K, RELA (v-*rel* riticuloendotheliosis viral oncogene, homolog A), NFkB1 (nuclear factor of kappa light chain polypeptide gene enhancer in B cells 1), and RAF 1 identified by GSEA support the conclusion that this cascade, which directs the downregulation of apoptosis,[35,38,39] is associated with differential outcome in our study.

Modulation of cell survival by the Ras signaling pathway has been shown to depend on cell type and level of gene expression.[38,40] However, the assessment of the transcriptional patterns within the total PBMC compartment cannot pinpoint causal processes within a particular cellular subcompartment or to a specific functional protein. Nevertheless, downregulation of apoptosis in the good outcome group, as assessed in the PBMC compartment, was associated with a statistically significant, fourfold less decline in $CD4^+$ T cells than observed in the poor outcome group. This observation is consistent with that of van Grevenynghe and colleagues, who reported that the central memory $CD4^+$ T cells of elite controllers were less susceptible to Fas-regulated apoptosis.[41] It is also important to note that persons with higher $CD4^+$ cell nadir while on ART exhibited a delayed time to the development of primary clinical end points in the study from which these samples were drawn.[6] Observations from the SMART study that addressed outcome during episodic antiretroviral therapy guided by $CD4^+$ T cell counts showed a significantly increased risk of opportunistic infections and death compared with continuous therapy, which was postulated to be due to a decline in $CD4^+$ T cells and concomitant increase in viral load.[24] Furthermore, that gene expression patterns associated with the downregulation of apoptosis in the good outcome group could be distinguished so early (week 0) may indicate that such patterns had been established prior to the cessation of ART.

The identification of a set of genes definitively associated with the downregulation of cell death as an attribute of the good outcome group is a reasonable point of departure for future studies on specific subpopulations of cells or in animal models that might confirm and extend our observations to specific cell types or tissues. Ultimately, candidate biomarkers such as these, determined in well controlled clinical studies in which the traditional makers of viral load and $CD4^+$ T cells are well characterized, will need to be evaluated in prospective clinical studies.

Acknowledgments

We thank M. Pochyla for expert technical laboratory work and Dr. Gustavo Kijak and Mr. Eric Sanders-Buell, all of the Henry M. Jackson Foundation, for advice on the design and execution of RT-PCR. We also thank Dr. Jerome Kim, Armed Forces Research Institute of the Medical Sciences, Bangkok, for helpful advice in the initial stages of this work and Dr. Emil Lesho, Walter Reed Army Institute of Research, for scrutiny of the final draft. This work was supported in part by Cooperative Agreement no. W81XWH-04-2-0005 between the U.S. Army Medical Research and Materiel Command and the Henry M. Jackson Foundation for the Advancement of Military Medicine. This work was supported by the Statistical and Data Management Center under the National Institute of Allergy and Infectious Disease grant no. 5U01 AI38855 and in part by the AIDS Clinical Trials Group funded by the National Institute of Allergy and Infectious Diseases grant no. AI-68636. The parent ACTG study from which these samples were derived, was funded by grants: AI025915, AI027666, AI27670, AI25897, AI25868, RR00046, AI50410, AI46386, RR00047, AI 27665, RR00096, AI 27664, AI46381, AI032783, AI045008, AI27660, AI46370, AI 27673, A125903, AI27658, RR00044, AI27661, AI39156, and AI25859.

References

1. Carpenter CC, Fischl MA, Hammer SM, *et al*. Antiretroviral therapy for HIV infection in 1997: updated recommendations of the International AIDS Society-USA panel. JAMA 1997;277:1962–1969.
2. Hammer SM, Saag MS, Schechter M, *et al*. Treatment for adult HIV infection: 2006 recommendations of the International AIDS Society-USA panel. JAMA 2006;296:827–843.
3. Boschi A. Tinelli C, Ortolani P, *et al*. CD4+ cell count guided treatment interruptions in chronic HIV infected patients with response to highly active antiretroviral therapy. AIDS 2004;18:2381–2389.
4. Ananworanich J, Gayet-Agenon A, LaBraz M, *et al*. CD4 guided scheduled treatment interruption compared to continuous therapy for patients infected with HIV-1: results of the Staccato randomized trial. Lancet 2006;368:459–465.
5. Cardiello PG, Hassink E, Ananworanich J, *et al*. A prospective randomized trial of structured treatment interruption for patients with chronic HIV type 1 infection. Clin Infect Dis 2005;40:594–600.
6. Skiest DJ, Su Z, Havlir DV, *et al*. Interruption of antiretroviral treatment in HIV-infected patients with preserved immune function is associated with a low rate of clinical progression: a prospective study by AIDS Clinical Trials Group 5170. J Infect Dis 2007;195:1426–1436.
7. Davey RT, Bhat N, Yoder C, *et al*. HIV-1 and T cell dynamics after interruption of highly active antiretroviral therapy

(HAART) in patients with a history of sustained viral suppression. Proc Natl Acad Sci U S A 1999;96:15109–15114.
8. Delaugerre C, Valantin MA, Mouroux M, *et al*. Re-occurrence of HIV-1 drug mutations after treatment re-initiation following interruption in patients with multiple treatment failure. AIDS 2001;15:2189–2191.
9. Miller V, Sabin C, Hertogs K, *et al*. Virological and immunological effects of treatment interruptions in HIV-1 infected patients with treatment failure. AIDS 2000;14: 2857–2867.
10. Kaufmann DE, Lichterfeld M, Altfeld M, *et al*. Limited durability of viral control following treated acute HIV infection. PLoS Med 2004;1:137–147.
11. Oxenius A, McLean, AR, Fischer M, *et al*. Human immunodeficiency virus specific CD8+ T cell responses do not predict viral growth and clearance rates during structured intermittent antiretroviral therapy. J Virol 2002;76:10169–10176.
12. Oxenius A, Price DA, Gunthard HF, *et al*. Stimulation of HIV specific cellular immunity by structured treatment interruption fails to enhance viral control in chronic HIV infection. Proc Natl Acad Sci U S A 2002;99:13747–13752.
13. Ortiz GM, Wellons M, Brancato J, *et al*. Structured antiretroviral treatment interruptions in chronically HIV-infected subjects. Proc Natl Acad Sci U S A 2001;98: 13288–13293.
14. Lempicki RA, Kovacs JA, Baseleer MW, et al. Impact of HIV-1 infection and highly active antiretroviral therapy on the kinetics of CD4+ and CD8+ T cell turnover in HIV-infected patients. Proc Natl Acad Sci U S A 2000;97:1377–13783.
15. Frost SDW, Martinez-Picado J, Ruiz L, Clotet B, and Leigh Brown AJ. Viral dynamics during structured treatment interruptions of chronic human immunodeficiency virus type 1 infection. J Virol 2002;76:968–979.
16. Ruiz L, Carcelain G, Martinez-Picado J, et al. HIV dynamics and T cell immunity after three structured treatment interruptions in chronic HIV-1 infection. AIDS 2001;15:F19–F27.
17. Garcia F, Plana M, Vidal C, et al. Dynamics of viral load rebound and immunological changes after stopping effective antiretroviral therapy. AIDS 1999;13:F79–F86.
18. Papasasvvas E, Kostman JR, Mounzer K, et al. Randomized, controlled trial of therapy interruption in chronic HIV-infection. PLoS Med 2004;1:218–228.
19. Molto J, Ruiz L, Romeu J, et al. Influence of prior structured treatment interruptions on the length of time without antiretroviral treatment in chronically HIV-infected subjects. AIDS Res Hum Retroviruses 2004;12:1283–1288.
20. Lawrence J, Mayers DL, Huppler-Hullsiek K, et al. Structured treatment interruption in patients with multidrug-resistant human immunodeficiency virus. New Engl J Med 2003; 349:837–846.
21. Steeck H, Jessen H, Alter G, et al. Immunological and virological impact of highly active antiretroviral therapy initiated during acute HIV-1 infection. J Infect Dis 2006;194: 734–739.
22. Schweighardt B, Ortiz GM, Grant RM, et al. Emergence of drug-resistant HIV-1 variants in patients undergoing structured treatment interruptions. AIDS 2002;16:2342–2344.
23. Koup RA. Reconsidering early HIV treatment and supervised treatment interruptions. PLoS Med 2004;1:109–110.
24. El-Sadr WM and Members of the SMART Study Group. CD4+ Count–Guided Interruption of Antiretroviral Treatment the Strategies for Management of Antiretroviral Therapy (SMART) Study Group. New Engl J Med 2006; 355: 2283–2296.
25. Vahey MT, Nau ME, Taubman M, et al. Patterns of gene expression in peripheral blood mononuclear cells of rhesus macaques infected with SIVmac251 and exhibiting differential rates of disease expression. AIDS Res Hum Retroviruses 2003;19:369–387.
26. Li C, Wong W. Model based analysis of oligonucleotide arrays: expression index computation and outlier detection. Proc Natl Acad Sci U S A 2001;98:31–36.
27. Irizarry RA, Bolstad BM, Collin F, et al. Summaries of Affymetrix GeneChip probe level data. Nucleic Acids Res 2003;31:e15.
28. Tusher VG, Tibshirani R, and Chu G. Significance analysis of microarrays applied to the ionizing radiation response. Proc Natl Acad Sci U S A 2001;98:5116–5121.
29. Dennis G, Sherman BT, Hosack DA, et al. DAVID: Database for annotation, visualization and integrated discovery. Genome Biol 2003;4:P3.
30. Tibshirani R, Hastie T, Narasimhan B, and Chu G. Diagnosis of multiple cancer types by shrunken centroids of gene expression. Proc Natl Acad Sci U S A 2002;99:6567–6572.
31. Silvestri G, Fedanov A, Germon S, *et al*. Divergent host responses during primary simian immunodeficiency virus SIVsm infection of natural sooty mangabey and nonnatural rhesus macaque hosts. J Virol 2005;79:4043–4054.
32. Choudhary SK, Vrisekoop N, Jansen CA, *et al*. Low immune activation despite high levels of pathogenic human immunodeficiency virus type 1 results in long term asymptomatic disease. J Virol 2007;81:8838–8842.
33. Vojtek AB and Der CJ. Increasing complexity of the Ras signaling pathway. J Biol Chem 1998;273:19925–19928.
34. Cox AD and Der CJ. The dark side of Ras: regulation of apoptosis. Oncogene 2003;22:8999–9006.
35. Kolch W. Meaningful relationships: the regulation of the Ras/Raf/MEK/ERK pathway by protein interactions. Biochem J 2000;351:289–305.
36. Chang F, Steelman LS, Shelton JG, *et al*. Regulation of cell cycle progression and apoptosis by the Ras/Raf/MEK/ERK pathway (review). Int J Oncol 2002;22:469–480.
37. Blum R and Kloog Y. Tailoring Ras pathway inhibitor combinations for cancer therapy. Drug Resist Updat 2005;8: 369–380.
38. Bonni A, Brunet A, West AE, Sandeep RD, Takasu MA, and Greenberg ME. Cell survival promoted by the Ras-MAPK signaling pathway by transcription dependent and independent mechanisms. Science 1999;286:1358–1362.
39. Downward J. Ras signaling and apoptosis. Curr Opin Genet Dev 1998;8:49–54.
40. Chen CY, Liou J, Forman LW, and Faller DV. Differential regulation of discrete apoptotic pathways by Ras. J Biol Chem 1998;273:16700–16709.
41. van Grevenynghe J, Procopio FA, He Z, *et al*. Transcription factor FOXO3a controls the persistence of memory CD4+ T cells during HIV infection. Nat Med 2008;14:266–274.

Address reprint requests to:
Maryanne T. Vahey, Ph.D.
Deputy Director
Division of Retrovirology
United States Military HIV Research Program
1600 East Gude Drive
Rockville, MD 20850

E-mail: mvahey@hivresearch.org

APPENDIX: FULL ANNOTATION INFORMATION FOR DIFFERENTIALLY EXPRESSED GENES

ProbesetIDs	*Symbols*	*PublicID*	*UniGeneID*	*Chromosome location*	*Gene title*
Good outcome group: 51 up regulated genes					
206486_at	LAG3	NM_002286	Hs.409523	chr12p13.32	Lymphocyte-activation gene 3
203554_x_at	PTTG1	NM_004219	Hs.350966	chr5q35.1	Pituitary tumor-transforming 1
202589_at	TYMS	NM_001071	Hs.592338	chr18p11.32	Thymidylate synthetase
200986_at	SERPING1	NM_000062	Hs.384598	chr11q12-q13.1	Serpin peptidase inhibitor, clade G (C1 inhibitor), member 1
209773_s_at	RRM2	BC001886	Hs.226390	chr2p25-p24	Ribonucleotide reductase M2 polypeptide
206666_at	GZMK	NM_002104	Hs.277937	chr5q11-q12	Granzyme K (granzyme 3; tryptase II)
218039_at	NUSAP1	NM_016359	Hs.615092	chr15q15.1	Nucleolar and spindle-associated protein 1
214453_s_at	IFI44	NM_006417	Hs.82316	chr1p31.1	Interferon-induced protein 44
207840_at	CD160	NM_007053	Hs.488237	chr1q21.1	CD160 molecule
206513_at	AIM2	NM_004833	Hs.281898	chr1q22	Absent in melanoma 2
204439_at	IFI44L	NM_006820	Hs.389724	chr1p31.1	Interferon-induced protein 44-like
205483_s_at	ISG15	NM_005101	Hs.458485	chr1p36.33	ISG15 ubiquitin-like modifier
200629_at	WARS	NM_004184	Hs.497599	chr14q32.31	Tryptophanyl-tRNA synthetase
204747_at	IFIT3	NM_001549	Hs.47338	chr10q24	Interferon-induced protein with tetratricopeptide repeats 3
204639_at	ADA	NM_000022	Hs.255479	chr20q12-q13.11	Adenosine deaminase
216615_s_at	HTR3A	AJ005205	Hs.413899	chr11q23.1	5-hydroxytryptamine (serotonin) receptor 3A
201649_at	UBE2L6	NM_004223	Hs.425777	chr11q12	Ubiquitin-conjugating enzyme E2L 6
204224_s_at	GCH1	NM_000161	Hs.86724	chr14q22.1-q22.2	GTP cyclohydrolase 1 (dopa-responsive dystonia)
217933_s_at	LAP3	NM_015907	Hs.570791	chr4p15.32	Leucine aminopeptidase 3
213060_s_at	CHI3L2	U58515	Hs.514840	chr1p13.3	Chitinase 3-like 2 /// chitinase 3-like 2
209040_s_at	PSMB8	U17496	Hs.180062	chr6p21.3	Proteasome (prosome, macropain) subunit, beta type, 8
200887_s_at	STAT1	NM_007315	Hs.651258	chr2q32.2	Signal transducer and activator of transcription 1, 91kDa
204246_s_at	DCTN3	NM_007234	Hs.511768	chr9p13	Dynactin 3 (p22)
202086_at	MX1	NM_002462	Hs.517307	chr21q22.3	Myxovirus (influenza virus) resistance 1
218400_at	OAS3	NM_006187	Hs.528634	chr12q24.2	2′-5′-oligoadenylate synthetase 3, 100kDa
203153_at	IFIT1	NM_001548	Hs.20315	chr10q25-q26	Interferon-induced protein with tetratricopeptide repeats 1
218943_s_at	DDX58	NM_014314	Hs.190622	chr9p12	DEAD (Asp-Glu-Ala-Asp) box polypeptide 58
205241_at	SCO2	NM_005138	Hs.567405	chr22q13.33	SCO cytochrome oxidase-deficient homolog 2 (yeast)
203232_s_at	ATXN1	NM_000332	Hs.434961	chr6p23	Ataxin 1
200814_at	PSME1	NM_006263	Hs.75348	chr14q11.2	Proteasome (prosome, macropain) activator subunit 1
201274_at	PSMA5	NM_002790	Hs.485246	chr1p13	Proteasome (prosome, macropain) subunit, alpha type, 5
206991_s_at	CCR5	NM_000579	Hs.450802	chr3p21.31	Chemokine (C-C motif) receptor 5
210046_s_at	IDH2	U52144	Hs.596461	chr15q26.1	Isocitrate dehydrogenase 2 (NADP+), mitochondrial
201762_s_at	PSME2	NM_002818	Hs.434081	chr14q11.2	Proteasome (prosome, macropain) activator subunit 2
215332_s_at	CD8B	AW296309	Hs.405667	chr2p12	CD8b molecule
204415_at	IFI6	NM_022873	Hs.523847	chr1p35	Interferon, alpha-inducible protein 6
202095_s_at	BIRC5	NM_001168	Hs.514527	chr17q25	Baculoviral IAP repeat-containing 5 (survivin)
200923_at	LGALS3BP	NM_005567	Hs.514535	chr17q25	Lectin, galactoside-binding, soluble, 3 binding protein
204655_at	CCL5	NM_002985	Hs.514821	chr17q11.2-q12	Chemokine (C-C motif) ligand 5
218350_s_at	GMNN	NM_015895	Hs.234896	chr6p22.2	Geminin, DNA replication inhibitor
209714_s_at	CDKN3	AF213033	Hs.84113	chr14q22	Cyclin-dependent kinase inhibitor 3
204173_at	MYL6B	NM_002475	Hs.632731	chr12q13.13	Myosin, light chain 6B, alkali, smooth muscle and non-muscle
200633_at	UBB	NM_018955	Hs.356190	chr17p12-p11.2	Ubiquitin B /// ubiquitin B

(*continued*)

APPENDIX: FULL ANNOTATION INFORMATION FOR DIFFERENTIALLY EXPRESSED GENES (*CONTINUED*)

ProbesetIDs	*Symbols*	*PublicID*	*UniGeneID*	*Chromosome location*	*Gene title*
44673_at	SIGLEC1	N53555	Hs.31869	chr20p13	Sialic acid binding Ig-like lectin 1, sialoadhesin
210243_s_at	B4GALT3	AF038661	Hs.321231	chr1q21-q23	UDP-Gal:betaGlcNAc beta 1,4-galactosyltransferase, polypeptide 3
200961_at	SEPHS2	NM_012248	Hs.118725	chr16p11.2	Selenophosphate synthetase 2
204798_at	MYB	NM_005375	Hs.531941	chr6q22-q23	V-myb myeloblastosis viral oncogene homolog (avian)
204279_at	PSMB9	NM_002800	Hs.132682	chr6p21.3	Proteasome (prosome, macropain) subunit, beta type, 9
215313_x_at	HLA-A	AA573862	Hs.181244	chr6p21.3	Major histocompatibility complex, class I, A
212203_x_at	IFITM3	BF338947	Hs.374650	chr11p15.5	Interferon induced transmembrane protein 3 (1-8U)
202411_at	IFI27	NM_005532	Hs.532634	chr14q32	Interferon, alpha-inducible protein 27
Poor outcome group: 133 upregulated genes					
214453_s_at	IFI44	NM_006417	Hs.82316	chr1p31.1	Interferon-induced protein 44
204439_at	IFI44L	NM_006820	Hs.389724	chr1p31.1	Interferon-induced protein 44-like
204747_at	IFIT3	NM_001549	Hs.47338	chr10q24	Interferon-induced protein with tetratricopeptide repeats 3
219863_at	HERC5	NM_016323	Hs.26663	chr4q22.1	Hect domain and RLD 5
203153_at	IFIT1	NM_001548	Hs.20315	chr10q25-q26	Interferon-induced protein with tetratricopeptide repeats 1
200986_at	SERPING1	NM_000062	Hs.384598	chr11q12-q13.1	Serpin peptidase inhibitor, clade G (C1 inhibitor), member 1
202748_at	GBP2	NM_004120	Hs.386567	chr1p22.2	Guanylate binding protein 2, interferon-inducible
205483_s_at	ISG15	NM_005101	Hs.458485	chr1p36.33	ISG15 ubiquitin-like modifier
218400_at	OAS3	NM_006187	Hs.528634	chr12q24.2	2′-5′-oligoadenylate synthetase 3, 100kDa
206486_at	LAG3	NM_002286	Hs.409523	chr12p13.32	Lymphocyte-activation gene 3
202086_at	MX1	NM_002462	Hs.517307	chr21q22.3	Myxovirus (influenza virus) resistance 1
200923_at	LGALS3BP	NM_005567	Hs.514535	chr17q25	Lectin, galactoside-binding, soluble, 3 binding protein
44673_at	SIGLEC1	N53555	Hs.31869	chr20p13	Sialic acid binding Ig-like lectin 1, sialoadhesin
202270_at	GBP1	NM_002053	Hs.62661	chr1p22.2	Guanylate binding protein 1, interferon-inducible
202145_at	LY6E	NM_002346	Hs.521903	chr8q24.3	Lymphocyte antigen 6 complex, locus E
205241_at	SCO2	NM_005138	Hs.567405	chr22q13.33	SCO cytochrome oxidase deficient homolog 2 (yeast)
201786_s_at	ADAR	NM_001111	Hs.12341	chr1q21.1-q21.2	Adenosine deaminase, RNA-specific
208436_s_at	IRF7	NM_004030	Hs.166120	chr11p15.5	Interferon regulatory factor 7
218039_at	NUSAP1	NM_016359	Hs.615092	chr15q15.1	Nucleolar and spindle-associated protein 1
204224_s_at	GCH1	NM_000161	Hs.86724	chr14q22.1-q22.2	GTP cyclohydrolase 1 (dopa-responsive dystonia)
218350_s_at	GMNN	NM_015895	Hs.234896	chr6p22.2	Geminin, DNA replication inhibitor
204415_at	IFI6	NM_022873	Hs.523847	chr1p35	Interferon, alpha-inducible protein 6
203358_s_at	EZH2	NM_004456	Hs.444082	chr7q35-q36	Enhancer of zeste homolog 2 (Drosophila)
204994_at	MX2	NM_002463	Hs.926	chr21q22.3	Myxovirus (influenza virus) resistance 2 (mouse)
203554_x_at	PTTG1	NM_004219	Hs.350966	chr5q35.1	Pituitary tumor-transforming 1
212203_x_at	IFITM3	BF338947	Hs.374650	chr11p15.5	Interferon induced transmembrane protein 3 (1-8U)
202411_at	IFI27	NM_005532	Hs.532634	chr14q32	Interferon, alpha-inducible protein 27
212185_x_at	MT2A	NM_005953	Hs.647371	chr16q13	Metallothionein 2A
201762_s_at	PSME2	NM_002818	Hs.434081	chr14q11.2	Proteasome (prosome, macropain) activator subunit 2 (PA28 beta)
206914_at	CRTAM	NM_019604	Hs.159523	chr11q22-q23	Cytotoxic and regulatory T cell molecule
206991_s_at	CCR5	NM_000579	Hs.450802	chr3p21.31	Chemokine (C-C motif) receptor 5
207840_at	CD160	NM_007053	Hs.488237	chr1q21.1	CD160 molecule

APPENDIX: FULL ANNOTATION INFORMATION FOR DIFFERENTIALLY EXPRESSED GENES (*CONTINUED*)

ProbesetIDs	*Symbols*	*PublicID*	*UniGeneID*	*Chromosome location*	*Gene title*
202589_at	TYMS	NM_001071	Hs.592338	chr18p11.32	Thymidylate synthetase
210797_s_at	OASL	AF063612	Hs.118633	chr12q24.2	2′-5′-oligoadenylate synthetase-like
206133_at	BIRC4BP	NM_017523	Hs.441975	chr17p13.2	XIAP associated factor-1
204655_at	CCL5	NM_002985	Hs.514821	chr17q11.2-q12	Chemokine (C-C motif) ligand 5
201649_at	UBE2L6	NM_004223	Hs.425777	chr11q12	Ubiquitin-conjugating enzyme E2L 6
204858_s_at	ECGF1	NM_001953	Hs.592212	chr22q13-22q13.33	Endothelial cell growth factor 1 (platelet-derived)
200629_at	WARS	NM_004184	Hs.497599	chr14q32.31	Tryptophanyl-tRNA synthetase
204204_at	SLC31A2	NM_001860	Hs.24030	chr9q31-q32	Solute carrier family 31 (copper transporters), member 2
216526_x_at	HLA-C	AK024836	Hs.77961	chr6p21.3	Major histocompatibility complex, class I, C
205692_s_at	CD38	NM_001775	Hs.479214	chr4p15	CD38 molecule
221485_at	B4GALT5	AL035683	Hs.370487	chr20q13.1-q13.2	UDP-Gal:betaGlcNAc beta 1,4-galactosyltransferase, polypeptide 5
218599_at	REC8L1	NM_005132	Hs.419259	chr14q11.2-q12	REC8-like 1 (yeast)
210046_s_at	IDH2	U52144	Hs.596461	chr15q26.1	Isocitrate dehydrogenase 2 (NADP+), mitochondrial
206513_at	AIM2	NM_004833	Hs.281898	chr1q22	Absent in melanoma 2
204211_x_at	EIF2AK2	NM_002759	Hs.131431	chr2p22-p21	Eukaryotic translation initiation factor 2-alpha kinase 2
200887_s_at	STAT1	NM_007315	Hs.651258	chr2q32.2	Signal transducer and activator of transcription 1, 91kDa
203052_at	C2	NM_000063	Hs.408903	chr6p21.3	Complement component 2
206461_x_at	MT1H	NM_005951	Hs.438462	chr16q13	Metallothionein 1H
217933_s_at	LAP3	NM_015907	Hs.570791	chr4p15.32	Leucine aminopeptidase 3
204972_at	OAS2	NM_016817	Hs.414332	chr12q24.2	2′-5′-oligoadenylate synthetase 2, 69/71kDa
202954_at	PAK3	NM_007019	Hs.93002	chrXq22.3-q23	p21 (CDKN1A)-activated kinase 3
202345_s_at	FABP5	NM_001444	Hs.632112	chr8q21.13	Fatty acid binding protein 5 (psoriasis-associated)
218943_s_at	DDX58	NM_014314	Hs.190622	chr9p12	DEAD (Asp-Glu-Ala-Asp) box polypeptide 58
202484_s_at	MBD2	AF072242	Hs.25674	chr18q21	Methyl-CpG binding domain protein 2
202953_at	C1QB	NM_000491	Hs.8986	chr1p36.12	Complement component 1, q subcomponent, B chain
201315_x_at	IFITM2	NM_006435	Hs.174195	chr11p15.5	Interferon induced transmembrane protein 2 (1-8D)
205552_s_at	OAS1	NM_002534	Hs.524760	chr12q24.1	2′,5′-oligoadenylate synthetase 1, 40/46kDa
209773_s_at	RRM2	BC001886	Hs.226390	chr2p25-p24	Ribonucleotide reductase M2 polypeptide
219684_at	RTP4	NM_022147	Hs.43388	chr3q27.3	Receptor (chemosensory) transporter protein 4
204533_at	CXCL10	NM_001565	Hs.632586	chr4q21	Chemokine (C-X-C motif) ligand 10
203350_at	AP1G1	NM_001128	Hs.461253	chr16q23	Adaptor-related protein complex 1, gamma 1 subunit
202107_s_at	MCM2	NM_004526	Hs.477481	chr3q21	MCM2 minichromosome maintenance deficient 2, mitotin (S. cerevisiae)
215313_x_at	HLA-A	AA573862	Hs.181244	chr6p21.3	Major histocompatibility complex, class I, A
201088_at	KPNA2	NM_002266	Hs.632749	chr17q23.1-q23.3	Karyopherin alpha 2 (RAG cohort 1, importin alpha 1)
210354_at	IFNG	M29383	Hs.856	chr12q14	Interferon, gamma
213475_s_at	ITGAL	AC002310	Hs.174103	chr16p11.2	Integrin, alpha L (antigen CD11A (p180)
35254_at	TRAFD1	AB007447	Hs.5148	chr12q	TRAF-type zinc finger domain containing 1
218662_s_at	NCAPG	NM_022346	Hs.567567	chr4p15.33	Non-SMC condensin I complex, subunit G
208683_at	CAPN2	M23254	Hs.350899	chr1q41-q42	Calpain 2, (m/II) large subunit
203344_s_at	RBBP8	NM_002894	Hs.546282	chr18q11.2	Retinoblastoma binding protein 8
203882_at	ISGF3G	NM_006084	Hs.1706	chr14q11.2	Interferon-stimulated transcription factor 3, gamma 48kDa

(*continued*)

APPENDIX: FULL ANNOTATION INFORMATION FOR DIFFERENTIALLY EXPRESSED GENES (*CONTINUED*)

ProbesetIDs	*Symbols*	*PublicID*	*UniGeneID*	*Chromosome location*	*Gene title*
203050_at	TP53BP1	NM_005657	Hs.440968	chr15q15-q21	Tumor protein p53 binding protein, 1
203258_at	DRAP1	NM_006442	Hs.356742	chr11q13.3	DR1-associated protein 1 (negative cofactor 2 alpha)
203455_s_at	SAT1	NM_002970	Hs.28491	chrXp22.1	Spermidine/spermine N1-acetyltransferase 1
203606_at	NDUFS6	NM_004553	Hs.408257	chr5p15.33	NADH dehydrogenase (ubiquinone) Fe-S protein 6, 13kDa
35974_at	LRMP	U10485	Hs.124922	chr12p12.1	Lymphoid-restricted membrane protein
205633_s_at	ALAS1	NM_000688	Hs.476308	chr3p21.1	Aminolevulinate, delta-, synthase 1
219209_at	IFIH1	NM_022168	Hs.163173	chr2p24.3-q24.3	Interferon induced with helicase C domain 1
207614_s_at	CUL1	NM_003592	Hs.146806	chr7q36.1	Cullin 1
216950_s_at	FCGR1A	X14355	Hs.77424	chr1q21.2-q21.3	Fc fragment of IgG, high-affinity Ia, receptor (CD64)
202446_s_at	PLSCR1	AI825926	Hs.130759	chr3q23	Phospholipid scramblase 1
214022_s_at	IFITM1	AA749101	Hs.458414	chr11p15.5	Interferon induced transmembrane protein 1 (9-27)
202863_at	SP100	NM_003113	Hs.369056	chr2q37.1	SP100 nuclear antigen
204146_at	RAD51AP1	BE966146	Hs.591046	chr12p13.2-p13.1	RAD51 associated protein 1
203236_s_at	LGALS9	NM_009587	Hs.81337	chr17q11.1	Lectin, galactoside-binding, soluble, 9 (galectin 9)
207181_s_at	CASP7	NM_001227	Hs.9216	chr10q25	Caspase 7, apoptosis-related cysteine peptidase
219938_s_at	PSTPIP2	NM_024430	Hs.567384	chr18q12	Proline-serine-threonine phosphatase interacting protein 2
203217_s_at	ST3GAL5	NM_003896	Hs.415117	chr2p11.2	ST3 beta-galactoside alpha-2,3-sialyltransferase 5
219212_at	HSPA14	NM_016299	Hs.534169	chr10p13	Heat shock 70kDa protein 14
204929_s_at	VAMP5	NM_006634	Hs.172684	chr2p11.2	Vesicle-associated membrane protein 5 (myobrevin)
243_g_at	MAP4	M64571	Hs.517949	chr3p21	Microtubule-associated protein 4
220966_x_at	ARPC5L	NM_030978	Hs.132499	chr9q33.3	Actin-related protein 2/3 complex, subunit 5-like
202735_at	EBP	NM_006579	Hs.30619	chrXp11.23-p11.22	Emopamil binding protein (sterol isomerase)
203805_s_at	FANCA	AW083279	Hs.567267	chr16q24.3	Fanconi anemia, complementation group A
204279_at	PSMB9	NM_002800	Hs.132682	chr6p21.3	Proteasome (prosome, macropain) subunit, beta type, 9
204175_at	ZNF593	NM_015871	—	chr1p36.11	Zinc finger protein 593
200814_at	PSME1	NM_006263	Hs.75348	chr14q11.2	Proteasome (prosome, macropain) activator subunit 1
204780_s_at	FAS	AA164751	Hs.244139	chr10q24.1	Fas (TNF receptor superfamily, member 6)
219159_s_at	SLAMF7	NM_021181	Hs.517265	chr1q23.1-q24.1	SLAM family member 7
219716_at	APOL6	NM_030641	Hs.257352	chr22q12.3	Apolipoprotein L, 6
205569_at	LAMP3	NM_014398	Hs.518448	chr3q26.3-q27	Lysosomal-associated membrane protein 3
219148_at	PBK	NM_018492	Hs.104741	chr8p21.2	PDZ binding kinase
207509_s_at	LAIR2	NM_002288	Hs.43803	chr19q13.4	Leukocyte-associated immunoglobulin-like receptor 2
221345_at	FFAR2	NM_005306	Hs.248056	chr19q13.1	Free fatty acid receptor 2
203755_at	BUB1B	NM_001211	Hs.631699	chr15q15	BUB1 budding uninhibited by benzimidazoles 1 homolog beta (yeast)
202702_at	TRIM26	NM_003449	Hs.485041	chr6p21.3	Tripartite motif-containing 26
221816_s_at	PHF11	BF055474	Hs.535080	chr13q14.3	PHD finger protein 11
202688_at	TNFSF10	NM_003810	Hs.478275	chr3q26	Tumor necrosis factor (ligand) superfamily, member 10
204639_at	ADA	NM_000022	Hs.255479	chr20q12-q13.11	Adenosine deaminase
204162_at	KNTC2	NM_006101	Hs.414407	chr18p11.32	Kinetochore associated 2
204804_at	TRIM21	NM_003141	Hs.632402	chr11p15.5	Tripartite motif-containing 21
203868_s_at	VCAM1	NM_001078	Hs.109225	chr1p32-p31	Vascular cell adhesion molecule 1

APPENDIX: FULL ANNOTATION INFORMATION FOR DIFFERENTIALLY EXPRESSED GENES (*CONTINUED*)

ProbesetIDs	*Symbols*	*PublicID*	*UniGeneID*	*Chromosome location*	*Gene title*
207375_s_at	IL15RA	NM_002189	Hs.524117	chr10p15-p14	Interleukin 15 receptor, alpha
219211_at	USP18	NM_017414	Hs.38260	chr22q11.21	Ubiquitin specific peptidase 18
206247_at	MICB	NM_005931	Hs.211580	chr6p21.3	MHC class I polypeptide-related sequence B
202870_s_at	CDC20	NM_001255	Hs.524947	chr1p34.1	Cell division cycle 20 homolog (S. cerevisiae)
208901_s_at	TOP1	J03250	Hs.592136	chr20q12-q13.1	Topoisomerase (DNA) I
209666_s_at	CHUK	AF080157	Hs.198998	chr10q24-q25	Conserved helix-loop-helix ubiquitous kinase
219607_s_at	MS4A4A	NM_024021	Hs.325960	chr11q12	Membrane-spanning 4-domains, subfamily A, member 4
206919_at	ELK4	NM_021795	Hs.497520	chr1q32	ELK4, ETS-domain protein (SRF accessory protein 1)
215171_s_at	TIMM17A	AK023063	Hs.20716	chr1q32.1	Translocase of inner mitochondrial membrane 17 homolog A (yeast)
202068_s_at	LDLR	NM_000527	Hs.213289	chr19p13.3	Low density lipoprotein receptor (familial hypercholesterolemia)
204009_s_at	KRAS	W80678	Hs.505033	chr12p12.1	v-Ki-ras2 Kirsten rat sarcoma viral oncogene homolog
205687_at	UBPH	NM_019116	Hs.3459	chr16p12	Ubiquitin-binding protein homolog
202087_s_at	CTSL	NM_001912	Hs.418123	chr9q21-q22	Cathepsin L
216598_s_at	CCL2	S69738	Hs.303649	chr17q11.2-q12	Chemokine (C-C motif) ligand 2
214933_at	CACNA1A	AA769818	Hs.501632	chr19p13.2-p13.1	Calcium channel, voltage-dependent, P/Q type, alpha 1A subunit
203420_at	FAM8A1	NM_016255	Hs.95260	chr6p22-p23	Family with sequence similarity 8, member A1
203964_at	NMI	NM_004688	Hs.54483	chr2p24.3-q21.3	N-myc (and STAT) interactor
208969_at	NDUFA9	AF050641	Hs.75227	chr12p13.3	NADH dehydrogenase (ubiquinone) 1 alpha subcomplex, 9, 39kDa
201664_at	SMC4	AL136877	Hs.58992	chr3q26.1	Structural maintenance of chromosomes 4
Poor outcome group: 208 downregulated genes					
201892_s_at	IMPDH2	NM_000884	Hs.476231	chr3p21.2	IMP (inosine monophosphate) dehydrogenase 2
211937_at	EIF4B	NM_001417	Hs.292063	chr12q13.13	Eukaryotic translation initiation factor 4B
200651_at	GNB2L1	NM_006098	Hs.5662	chr5q35.3	Guanine nucleotide binding protein (G protein)
203685_at	BCL2	NM_000633	Hs.150749	chr18q21.33	B-cell CLL/lymphoma 2
221476_s_at	RPL15	AF279903	Hs.381219	chr3p24.2	Ribosomal protein L15
218253_s_at	LGTN	NM_006893	Hs.497581	chr1q31-q32	Ligatin
200005_at	EIF3S7	NM_003753	Hs.55682	chr22q13.1	Eukaryotic translation initiation factor 3, subunit 7 zeta
219452_at	DPEP2	NM_022355	Hs.372633	chr16q22.1	Dipeptidase 2
205019_s_at	VIPR1	NM_004624	Hs.348500	chr3p22	Vasoactive intestinal peptide receptor 1
210908_s_at	PFDN5	AB055804	—	chr12q12	Prefoldin subunit 5
214167_s_at	RPLP0	AA555113	Hs.448226	chr12q24.2	Ribosomal protein, large, P0
205259_at	NR3C2	NM_000901	Hs.163924	chr4q31.1	Nuclear receptor subfamily 3, group C, member 2
210027_s_at	APEX1	M80261	Hs.73722	chr14q11.2-q12	APEX nuclease (multifunctional DNA repair enzyme) 1
200089_s_at	RPL4	AI953886	Hs.644628	chr15q22	Ribosomal protein L4
201433_s_at	PTDSS1	NM_014754	Hs.292579	chr8q22	Phosphatidylserine synthase 1
220755_s_at	C6orf48	NM_016947	Hs.640836	chr6p21.3	Chromosome 6 open reading frame 48
200705_s_at	EEF1B2	NM_001959	Hs.421608	chr2q33-q34	Eukaryotic translation elongation factor 1 beta 2
200024_at	RPS5	NM_001009	Hs.378103	chr19q13.4	Ribosomal protein S5
201064_s_at	PABPC4	NM_003819	Hs.169900	chr1p32-p36	Poly(A) binding protein, cytoplasmic 4 (inducible form)
218997_at	POLR1E	NM_022490	Hs.591087	chr9p13.2	Polymerase (RNA) I polypeptide E, 53kDa
210715_s_at	SPINT2	AF027205	Hs.31439	chr19q13.1	Serine peptidase inhibitor, Kunitz type, 2

(*continued*)

APPENDIX: FULL ANNOTATION INFORMATION FOR DIFFERENTIALLY EXPRESSED GENES (*CONTINUED*)

ProbesetIDs	*Symbols*	*PublicID*	*UniGeneID*	*Chromosome location*	*Gene title*
202283_at	SERPINF1	NM_002615	Hs.645378	chr17p13.1	Serpin peptidase inhibitor, clade F (alpha-2 antiplasmin
200937_s_at	RPL5	NM_000969	Hs.532359	chr1p22.1	Ribosomal protein L5
216520_s_at	TPT1	AF072098	Hs.374596	chr13q12-q14	Tumor protein, translationally controlled 1
219549_s_at	RTN3	NM_006054	Hs.473761	chr11q13	Reticulon 3
219922_s_at	LTBP3	NM_021070	Hs.289019	chr11q12	Latent transforming growth factor beta binding protein 3
219892_at	TM6SF1	NM_023003	Hs.513094	chr15q24-q26	Transmembrane 6 superfamily member 1
208631_s_at	HADHA	U04627	Hs.516032	chr2p23	Hydroxyacyl-coenzyme A dehydrogenase
218495_at	UXT	NM_004182	Hs.172791	chrXp11.23-p11.22	Ubiquitously-expressed transcript
206559_x_at	EEF1A1	NM_001403	—	chr6q14.1	Eukaryotic translation elongation factor 1 alpha 1
200858_s_at	RPS8	NM_001012	Hs.512675	chr1p34.1-p32	Ribosomal protein S8
217747_s_at	RPS9	NM_001013	Hs.546288	chr19q13.4	Ribosomal protein S9
206760_s_at	FCER2	NM_002002	Hs.465778	chr19p13.3	Fc fragment of IgE, low affinity II, receptor for (CD23)
200032_s_at	RPL9	NM_000661	Hs.513083	chr4p13	Ribosomal protein L9 /// ribosomal protein L9
201258_at	RPS16	NM_001020	Hs.397609	chr19q13.1	Ribosomal protein S16
205987_at	CD1C	NM_001765	Hs.132448	chr1q22-q23	CD1c molecule
206492_at	FHIT	NM_002012	Hs.196981	chr3p14.2	Fragile histidine triad gene
222212_s_at	LASS2	AK001105	Hs.643565	chr1q21.2	LAG1 homolog, ceramide synthase 2 (*S. cerevisiae*)
204153_s_at	MFNG	NM_002405	Hs.517603	chr22q12	MFNG O-fucosylpeptide 3-beta-N-acetylglucosaminyltransferase
216032_s_at	ERGIC3	AF091085	Hs.472558	chr20pter-q12	ERGIC and golgi 3
218084_x_at	FXYD5	NM_014164	Hs.333418	chr19q12-q13.1	FXYD domain containing ion transport regulator 5
207339_s_at	LTB	NM_002341	Hs.376208	chr6p21.3	Lymphotoxin beta (TNF superfamily, member 3)
201276_at	RAB5B	AF267863	Hs.567328	chr12q13	RAB5B, member RAS oncogene family
206337_at	CCR7	NM_001838	Hs.370036	chr17q12-q21.2	Chemokine (C-C motif) receptor 7 /// chemokine (C-C motif) receptor 7
221558_s_at	LEF1	AF288571	Hs.555947	chr4q23-q25	Lymphoid enhancer binding factor 1
214437_s_at	SHMT2	NM_005412	Hs.75069	chr12q12-q14	Serine hydroxymethyltransferase 2 (mitochondrial)
203233_at	IL4R	NM_000418	Hs.513457	chr16p11.2-12.1	Interleukin 4 receptor
200909_s_at	RPLP2	NM_001004	—	chr11p15.5-p15.4	Ribosomal protein, large, P2
203787_at	SSBP2	NM_012446	Hs.102735	chr5q14.1	Single-stranded DNA binding protein 2
208754_s_at	NAP1L1	AL162068	Hs.524599	chr12q21.2	Nucleosome assembly protein 1-like 1
210189_at	HSPA1L	D85730	Hs.558337	chr6p21.3	Heat shock 70kDa protein 1-like
200082_s_at	RPS7	AI805587	Hs.534346	chr2p25	Ribosomal protein S
200034_s_at	RPL6	NM_000970	Hs.528668	chr12q24.1	Ribosomal protein L6
201050_at	PLD3	NM_012268	Hs.257008	chr19q13.2	Phospholipase D family, member 3
203385_at	DGKA	NM_001345	Hs.524488	chr12q13.3	Diacylglycerol kinase, alpha 80 kDa
200010_at	RPL11	NM_000975	Hs.388664	chr1p36.1-p35	Ribosomal protein L11
203509_at	SORL1	NM_003105	Hs.368592	chr11q23.2-q24.2	Sortilin-related receptor, L(DLR class) A repeats-containing
200652_at	SSR2	NM_003145	Hs.74564	chr1q21-q23	Signal sequence receptor
201136_at	PLP2	NM_002668	Hs.77422	chrXp11.23	Proteolipid protein 2 (colonic epithelium-enriched)
210949_s_at	EIF3S8	BC000533	Hs.535464	chr16p11.2	Eukaryotic translation initiation factor 3, subunit 8
212191_x_at	RPL13	AW574664	Hs.410817	chr16q24.3	Ribosomal protein L13
209368_at	EPHX2	AF233336	Hs.212088	chr8p21-p12	Epoxide hydrolase 2, cytoplasmic
208697_s_at	EIF3S6	BC000734	Hs.405590	chr8q22-q23	Eukaryotic translation initiation factor 3, subunit 6 48 kDa
208764_s_at	ATP5G2	D13119	Hs.524464	chr12q13.13	ATP synthase, H+ transporting, mitochondrial F0 complex, subunit C2 (subunit 9)

APPENDIX: FULL ANNOTATION INFORMATION FOR DIFFERENTIALLY EXPRESSED GENES (*CONTINUED*)

ProbesetIDs	*Symbols*	*PublicID*	*UniGeneID*	*Chromosome location*	*Gene title*
200823_x_at	RPL29	NM_000992	Hs.425125	chr3p21.3-p21.2	Ribosomal protein L29
200936_at	RPL8	NM_000973	Hs.178551	chr8q24.3	Ribosomal protein L8
201106_at	GPX4	NM_002085	Hs.433951	chr19p13.3	Glutathione peroxidase 4 (phospholipid hydroperoxidase)
203413_at	NELL2	NM_006159	Hs.505326	chr12q13.11-q13.12	NEL-like 2 (chicken)
203818_s_at	SF3A3	NM_006802	Hs.77897	chr1p34.3	Splicing factor 3a, subunit 3, 60 kDa
200081_s_at	RPS6	BE741754	Hs.408073	chr9p21	Ribosomal protein S6 /// ribosomal protein S6
217860_at	NDUFA10	NM_004544	Hs.277677	chr2q37.3	NADH dehydrogenase (ubiquinone) 1 alpha subcomplex
208771_s_at	LTA4H	J02959	Hs.524648	chr12q22	Leukotriene A4 hydrolase
219528_s_at	BCL11B	NM_022898	Hs.510396	chr14q32.2	B-cell CLL/lymphoma 11B (zinc finger protein)
221593_s_at	RPL31	BC001663	Hs.469473	chr2q11.2	Ribosomal protein L31
201812_s_at	TOMM7	NM_019059	Hs.380920	chr7p15.3	Translocase of outer mitochondrial membrane 7 homolog (yeast)
200023_s_at	EIF3S5	NM_003754	Hs.516023	chr11p15.4	Eukaryotic translation initiation factor 3, subunit 5 epsilon
39318_at	TCL1A	X82240	Hs.2484	chr14q32.1	T-cell leukemia/lymphoma 1A
203547_at	CD4	U47924	Hs.631659	chr12pter-p12	CD4 molecule /// CD4 molecule
207895_at	NAALADL1	NM_005468	Hs.13967	chr11q12	N-acetylated alpha-linked acidic dipeptidase-like 1
203113_s_at	EEF1D	NM_001960	Hs.333388	chr8q24.3	Eukaryotic translation elongation factor 1 delta
200717_x_at	RPL7	NM_000971	Hs.571841	chr8q21.11	Ribosomal protein L7
208703_s_at	APLP2	BG427393	Hs.370247	chr11q23-q25	Amyloid beta (A4) precursor-like protein 2
213093_at	PRKCA	AI471375	Hs.531704	chr17q22-q23.2	Protein kinase C, alpha
200695_at	PPP2R1A	NM_014225	Hs.467192	chr19q13.33	Protein phosphatase 2 (formerly 2A)
202179_at	BLMH	NM_000386	Hs.371914	chr17q11.2	Bleomycin hydrolase
200817_x_at	RPS10	NM_001014	Hs.645317	chr6p21.31	Ribosomal protein S10
200965_s_at	ABLIM1	NM_006720	Hs.438236	chr10q25	Actin binding LIM protein 1
201005_at	CD9	NM_001769	Hs.114286	chr12p13.3	CD9 molecule
209504_s_at	PLEKHB1	AF081583	Hs.445489	chr11q13.5-q14.1	Pleckstrin homology domain containing
200933_x_at	RPS4X	NM_001007	Hs.446628	chrXq13.1	Ribosomal protein S4, X-linked
204949_at	ICAM3	NM_002162	Hs.75516	chr19p13.3-p13.2	Intercellular adhesion molecule 3
213762_x_at	RBMX	AI452524	Hs.380118	chrXq26.3	RNA binding motif protein, X-linked
203581_at	RAB4A	BC002438	Hs.296169	chr1q42-q43	RAB4A, member RAS oncogene family
217846_at	QARS	NM_005051	Hs.79322	chr3p21.3-p21.1	Glutaminyl-tRNA synthetase
202862_at	FAH	NM_000137	Hs.73875	chr15q23-q25	Fumarylacetoacetate hydrolase (fumarylacetoacetase)
205039_s_at	IKZF1	NM_006060	Hs.488251	chr7p13-p11.1	IKAROS family zinc finger 1 (Ikaros)
200008_s_at	GDI2	D13988	Hs.299055	chr10p15	GDP dissociation inhibitor 2 /// GDP dissociation inhibitor 2
210786_s_at	FLI1	M93255	Hs.504281	chr11q24.1-q24.3	Friend leukemia virus integration 1
204777_s_at	MAL	NM_002371	Hs.80395	chr2cen-q13	Mal, T-cell differentiation protein
209264_s_at	TSPAN4	AF054841	Hs.437594	chr11p15.5	Tetraspanin 4
200736_s_at	GPX1	NM_000581	Hs.76686	chr3p21.3	Glutathione peroxidase 1
201417_at	SOX4	AL136179	Hs.643910	chr6p22.3	SRY (sex determining region Y)-box 4
203088_at	FBLN5	NM_006329	Hs.332708	chr14q32.1	Fibulin 5
200036_s_at	RPL10A	NM_007104	Hs.546269	chr6p21.3-p21.2	Ribosomal protein L10a
200053_at	SPAG7	NM_004890	Hs.90436	chr17p13.2	Sperm associated antigen 7
200018_at	RPS13	NM_001017	Hs.446588	chr11p15	Ribosomal protein S13
212271_at	MAPK1	AA195999	Hs.431850	chr22q11.2	Mitogen-activated protein kinase 1
200763_s_at	RPLP1	NM_001003	Hs.356502	chr15q22	Ribosomal protein, large, P1
208822_s_at	DAP3	U18321	Hs.516746	chr1q21-q22	Death associated protein 3
214470_at	KLRB1	NM_002258	Hs.169824	chr12p13	Killer cell lectin-like receptor subfamily B, member 1
217969_at	C11orf2	NM_013265	Hs.277517	chr11q13	Chromosome 11 open reading frame2
220753_s_at	CRYL1	NM_015974	Hs.370703	chr13q12.11	Crystallin, lambda 1
200602_at	APP	NM_000484	Hs.651215	chr21q21.2-21q21.3	Amyloid beta (A4) precursor protein (peptidase nexin-II, Alzheimer disease)

(*continued*)

APPENDIX: FULL ANNOTATION INFORMATION FOR DIFFERENTIALLY EXPRESSED GENES (*CONTINUED*)

ProbesetIDs	*Symbols*	*PublicID*	*UniGeneID*	*Chromosome location*	*Gene title*
206343_s_at	NRG1	NM_013959	Hs.453951	chr8p21-p12	Neuregulin 1
203723_at	ITPKB	NM_002221	Hs.528087	chr1q42.13	Inositol 1,4,5-trisphosphate 3-kinase B
219700_at	PLXDC1	NM_020405	Hs.125036	chr17q21.1	Plexin domain containing 1
200099_s_at	RPS3A	AL356115	Hs.356572	chr4q31.2-q31.3	Ribosomal protein S3A
200013_at	RPL24	NM_000986	Hs.477028	chr3q12	Ribosomal protein L24 /// ribosomal protein L24
201256_at	COX7A2L	NM_004718	Hs.339639	chr2p21	Cytochrome c oxidase subunit VIIa polypeptide 2 like
200716_x_at	RPL13A	NM_012423	Hs.523185	chr19q13.3	Ribosomal protein L13a
208591_s_at	PDE3B	NM_000922	Hs.445711	chr11p15.1	Phosphodiesterase 3B, cGMP-inhibited
204612_at	PKIA	NM_006823	Hs.433700	chr8q21.12	Protein kinase (cAMP-dependent, catalytic) inhibitor alpha
217989_at	HSD17B11	NM_016245	Hs.282984	chr4q22.1	Hydroxysteroid (17-beta) dehydrogenase 11
204628_s_at	ITGB3	NM_000212	Hs.218040	chr17q21.32	Integrin, beta 3 (platelet glycoprotein IIIa, antigen CD61)
201968_s_at	PGM1	NM_002633	Hs.1869	chr1p31	Phosphoglucomutase 1
212063_at	CD44	BE903880	Hs.502328	chr11p13	CD44 molecule (Indian blood group)
218918_at	MAN1C1	NM_020379	Hs.197043	chr1p35	Mannosidase, alpha, class 1C, member 1
200093_s_at	HINT1	N32864	Hs.483305	chr5q31.2	Histidine triad nucleotide binding protein 1
206220_s_at	RASA3	NM_007368	Hs.369188	chr13q34	RAS p21 protein activator 3
221564_at	PRMT2	AL570294	Hs.154163	chr21q22.3	Protein arginine methyltransferase 2
220948_s_at	ATP1A1	NM_000701	Hs.371889	chr1p21	ATPase, Na+/K+ transporting, alpha 1 polypeptide
211954_s_at	RANBP5	BC000947	Hs.643743	chr13q32.2	RAN binding protein 5
201350_at	FLOT2	NM_004475	Hs.514038	chr17q11-q12	Flotillin 2
202554_s_at	GSTM3	AL527430	Hs.2006	chr1p13.3	Glutathione S-transferase M3 (brain)
221494_x_at	EIF3S12	AF085358	Hs.314359	chr19q13.2	Eukaryotic translation initiation factor 3, subunit 12
200962_at	RPL31	AI348010	Hs.647888	chr2q11.2	Ribosomal protein L31
201030_x_at	LDHB	NM_002300	Hs.446149	chr12p12.2-p12.1	Lactate dehydrogenase B
200644_at	MARCKSL1	NM_023009	Hs.75061	chr1p35.1	MARCKS-like 1
204490_s_at	CD44	M24915	Hs.502328	chr11p13	CD44 molecule (Indian blood group)
204718_at	EPHB6	NM_004445	Hs.380089	chr7q33-q35	EPH receptor B6
210978_s_at	TAGLN2	BC002616	Hs.517168	chr1q21-q25	Transgelin 2
208852_s_at	CANX	AI761759	Hs.651169	chr5q35	Calnexin
220606_s_at	C17orf48	NM_020233	Hs.47668	chr17p13.1	Chromosome 17 open reading frame 48
206674_at	FLT3	NM_004119	Hs.507590	chr13q12	Fms-related tyrosine kinase 3
204102_s_at	EEF2	NM_001961	Hs.515070	chr19pter-q12	Eukaryotic translation elongation factor 2
202247_s_at	MTA1	BE561596	Hs.525629	chr14q32.3	Metastasis associated 1
208692_at	RPS3	U14990	Hs.334176	chr11q13.3-q13.5	Ribosomal protein S3
200094_s_at	EEF2	AI004246	Hs.515070	chr19pter-q12	Eukaryotic translation elongation factor 2
217990_at	GMPR2	NM_016576	Hs.368855	chr14q12	Guanosine monophosphate reductase 2
200012_x_at	RPL21	NM_000982	Hs.632169	chr13q12.2	Ribosomal protein L21
200057_s_at	NONO	NM_007363	Hs.533282	chrXq13.1	Non-POU domain containing, octamer-binding
208796_s_at	CCNG1	BC000196	Hs.79101	chr5q32-q34	Cyclin G1
215739_s_at	TUBGCP3	AJ003062	Hs.224152	chr13q34	Tubulin, gamma complex associated protein 3
208478_s_at	BAX	NM_004324	Hs.631546	chr19q13.3-q13.4	BCL2-associated X protein
200674_s_at	RPL32	NM_000994	Hs.265174	chr3p25-p24	Ribosomal protein L32
208645_s_at	RPS14	AF116710	Hs.381126	chr5q31-q33	Ribosomal protein S14
212032_s_at	PTOV1	AL046054	—	chr19q13.33	Prostate tumor overexpressed gene 1
218338_at	PHC1	NM_004426	Hs.305985	chr12p13	Polyhomeotic homolog 1 (Drosophila)
201432_at	CAT	NM_001752	Hs.502302	chr11p13	Catalase
202731_at	PDCD4	NM_014456	Hs.232543	chr10q24	Programmed cell death 4 (neoplastic transformation inhibitor)
201118_at	PGD	NM_002631	Hs.464071	chr1p36.3-p36.13	Phosphogluconate dehydrogenase
212642_s_at	HIVEP2	AL023584	Hs.510172	chr6q23-q24	Human immunodeficiency virus type I enhancer binding protein 2

APPENDIX: FULL ANNOTATION INFORMATION FOR DIFFERENTIALLY EXPRESSED GENES (*CONTINUED*)

ProbesetIDs	*Symbols*	*PublicID*	*UniGeneID*	*Chromosome location*	*Gene title*
202736_s_at	LSM4	AA112507	Hs.515255	chr19p13.11	LSM4 homolog, U6 small nuclear RNA associated (S. cerevisiae)
208768_x_at	RPL22	D17652	Hs.515329	chr1p36.3-p36.2	Ribosomal protein L22
201049_s_at	RPS18	NM_022551	Hs.627414	chr6p21.3	Ribosomal protein S18
200074_s_at	RPL14	U16738	Hs.446522	chr3p22-p21.2	Ribosomal protein L14
65588_at	LOC388796	AA827892	Hs.400876	chr20q11.23	Hypothetical LOC388796
206686_at	PDK1	NM_002610	Hs.470633	chr2q31.1	Pyruvate dehydrogenase kinase, isozyme 1
200022_at	RPL18	NM_000979	Hs.515517	chr19q13	Ribosomal protein L18 /// ribosomal protein L18
201622_at	SND1	NM_014390	Hs.122523	chr7q31.3	Staphylococcal nuclease and tudor domain containing 1
217870_s_at	CMPK	NM_016308	Hs.11463	chr1p32	Cytidylate kinase
220773_s_at	GPHN	NM_020806	Hs.208765	chr14q23.3	Gephyrin
200804_at	TEGT	NM_003217	Hs.35052	chr12q12-q13	Testis enhanced gene transcript (BAX inhibitor 1)
202105_at	IGBP1	NM_001551	Hs.496267	chrXq13.1-q13.3	Immunoglobulin (CD79A) binding protein 1
200061_s_at	RPS24	BC000523	Hs.356794	chr10q22-q23	Ribosomal protein S24 /// ribosomal protein S24
200095_x_at	RPS10	AA320764	Hs.645317	chr6p21.31	ribosomal protein S10 /// ribosomal rotein S10
204892_x_at	EEF1A1	NM_001402	Hs.586423	chr6q14.1	Eukaryotic translation elongation factor 1 alpha 1
202213_s_at	CUL4B	AI650819	Hs.102914	chrXq23	Cullin 4B
200002_at	RPL35	NM_007209	Hs.182825	chr9q34.1	Ribosomal protein L35 /// ribosomal protein L35
200990_at	TRIM28	NM_005762	Hs.467408	chr19q13.4	Tripartite motif-containing 28
203865_s_at	ADARB1	NM_015833	Hs.474018	chr21q22.3	Adenosine deaminase, RNA-specific, B1 (RED1 homolog rat)
220001_at	PADI4	NM_012387	Hs.522969	chr1p36.13	Peptidyl arginine deiminase, type IV
215813_s_at	PTGS1	S36219	Hs.201978	chr9q32-q33.3	Prostaglandin-endoperoxide synthase 1
208700_s_at	TKT	L12711	Hs.89643	chr3p14.3	Transketolase (Wernicke-Korsakoff syndrome)
202990_at	PYGL	NM_002863	Hs.282417	chr14q21-q22	Phosphorylase, glycogen
212716_s_at	EIF3S12	AW083133	Hs.314359	chr19q13.2	Eukaryotic translation initiation factor 3, subunit 12
209185_s_at	IRS2	AF073310	Hs.442344	chr13q34	Insulin receptor substrate 2
221989_at	RPL10	AW057781	Hs.534404	chrXq28	Ribosomal protein L10
214359_s_at	HSP90AB1	AI218219	Hs.509736	chr6p12	Heat shock protein 90kDa alpha (cytosolic), class B member 1
201393_s_at	IGF2R	NM_000876	Hs.487062	chr6q26	Insulin-like growth factor 2 receptor
201257_x_at	RPS3A	NM_001006	Hs.356572	chr4q31.2-q31.3	Ribosomal protein S3A
205408_at	MLLT10	NM_004641	Hs.30385	chr10p12	Myeloid/lymphoid or mixed-lineage leukemia (trithorax homolog, Drosophila)
218679_s_at	VPS28	NM_016208	Hs.418175	chr8q24.3	Vacuolar protein sorting 28 homolog (*S. cerevisiae*)
202096_s_at	TSPO	NM_000714	Hs.202	chr22q13.31	Translocator protein (18 kDa)
211558_s_at	DHPS	U26266	Hs.79064	chr19p13.2-p13.1	Deoxyhypusine synthase
205055_at	ITGAE	NM_002208	Hs.513867	chr17p13	Integrin, alpha E (antigen CD103, human mucosal lymphocyte antigen 1
204867_at	GCHFR	NM_005258	Hs.631717	chr15q15	GTP cyclohydrolase I feedback regulator
200971_s_at	SERP1	NM_014445	Hs.518326	chr3q25.1	Stress-associated endoplasmic reticulum protein 1
203579_s_at	SLC7A6	AI660619	Hs.334848	chr16q22.1	Solute carrier family 7 (cationic amino acid transporter, y+ system), member 6
39249_at	AQP3	AB001325	Hs.234642	chr9p13	Aquaporin 3 (Gill blood group)
203408_s_at	SATB1	NM_002971	Hs.517717	chr3p23	Special AT-rich sequence binding protein 1
204454_at	LDOC1	NM_012317	Hs.45231	chrXq27	Leucine zipper, down-regulated in cancer 1

(*continued*)

APPENDIX: FULL ANNOTATION INFORMATION FOR DIFFERENTIALLY EXPRESSED GENES (*CONTINUED*)

ProbesetIDs	*Symbols*	*PublicID*	*UniGeneID*	*Chromosome location*	*Gene title*
205026_at	STAT5B	NM_012448	Hs.632256	chr17q11.2	Signal transducer and activator of transcription 5B
212257_s_at	SMARCA2	AW131754	Hs.298990	chr9p22.3	SWI/SNF related, matrix associated
220500_s_at	RABL2B	NM_007082	Hs.446425	chr22q13.33	RAB, member of RAS oncogene family-like 2B
212400_at	FAM102A	AL043266	Hs.568044	chr9q34.11	Family with sequence similarity 102, member A
202974_at	MPP1	NM_002436	Hs.496984	chrXq28	Membrane protein, palmitoylated 1, 55 kDa
213566_at	RNASE6	NM_005615	Hs.23262	chr14q11.2	Ribonuclease, RNase A family